

Study on Effect of Weld Cooling Rate on Fusion Zone Microstructure and Solidification Cracks in 316L Austenitic Stainless Steel

R. Sai Santhosh^{1a}, M. Aravind^{2a}, M. Divya^{3b}, A.K. Lakshminarayanan^{4a} and Shaju K. Albert^{5b}

^a Department of Mechanical Engineering, SSN College of Engineering, Kalavakkam - 603 110, India

^b Metallurgy and Materials Group, IGCAR, Kalpakkam - 603 102, India

Email: ¹sai14089@mech.ssn.edu.in; ²aravind14009@mech.ssn.edu.in;

³divya_mjs@igcar.gov.in; ⁴lakshminarayananak@ssn.edu.in; ⁵shaju@igcar.gov.in



DOI : 10.22486/iwj/2019/v52/i1/178271

ABSTRACT

A study on effect of cooling rate on mode of solidification and microstructure was carried out on austenitic stainless steel welds. A tube and plug of 316L stainless steel was joined using Gas Tungsten Arc Welding (GTAW) and laser welding processes. The welds were characterized using optical and Scanning Electron Microscope (SEM). The results indicate that cooling rate of the weld has significant effect on solidification mode, microstructure and solidification cracking. 316L weld joints prepared using GTAW process shows duplex microstructure of vermicular ferrite and austenite in the fusion zone. Whereas, the fusion zone of laser joint shows only single phase austenite microstructure. From these observations, it is clearly understood that the changes observed in the fusion zone microstructures of GTAW and laser welds are due to change in the mode of solidification as a result of change in the weld cooling rates. The predicted mode of solidification for GTA welds for 316L composition used in this study was Austenite-Ferrite (AF) and it was also confirmed through the microstructural observations. In laser joint, the weld has solidified in fully austenitic mode which deviates from the mode of solidification predicted by the conventional constitutional diagrams and hence modified weldability diagram was used. From this investigation, it was also found that the rapid solidification during laser welding is not completely partition less because segregation of sulphur was found using Scanning Electron Microscope – Energy Dispersive Spectroscopy (SEM-EDS) along the dendrite boundaries of laser welds. High cooling rate during weld solidification which influences fully austenitic mode of solidification and micro segregation of impurities along the grain boundaries contribute to solidification cracking of welds in laser joints.

Keywords: Solidification mode; solidification cracking; cooling rate; energy dispersive spectroscopy; laser welding; gas tungsten arc welding.

1.0 INTRODUCTION

AISI type 316L, a modified version of 316 austenite stainless steels with low carbon content (<0.03wt.%) is presently used as a structural material in fast nuclear reactors because of its better high temperature mechanical properties. One of the major problems encountered during the fabrication of this type of steel is its susceptibility to distortion and hot cracking [1]. Traditionally, Gas Tungsten Arc Welding (GTAW) has been used

for joining thin components of austenitic stainless steel. In spite of its wide usage, it has the complexity like tungsten electrode alignment, wide heat-affected-zone (HAZ) and a large heat input than required for welding very thin walled components [2]. Hence, a process that could reduce the heat input and thereby the size of the fusion zone and HAZ would be a better choice for welding thin sections than the GTAW process. Laser Beam Welding (LBW) is one such process which

is actively being considered as an alternative to GTAW process. LBW is a high power density process due to which full penetration welds have been made feasible with low heat input. Moreover, LBW is capable of producing a narrow HAZ with low residual stress and thereby reducing the distortions in the welded components [3]. Laser welding has a high cooling rate due to which it gives a fine grained microstructure and improved mechanical properties [4]. Rapid solidification of materials produces microstructures which significantly differ from that of conventional solidification [5]. So far there has not been a comparative study on laser and GTA welds prepared from the same steel composition pertaining to their solidification mode or cracking sensitivity. The present study has been carried out on the practically important tube to end plug joints which involve thin-to-thick joint configuration. The weld solidification structures of GTAW and laser welded joints have been comparatively studied to bring out the effect of cooling rate on solidification microstructures of SS316L weld joints and its impact on solidification cracking.

2.0 EXPERIMENTAL PROCEDURE

2.1 Material

In this study, 316L stainless steel tube of 20 mm outer diameter and 1 mm wall thickness and 316L end plug of the geometry given in **Fig. 1** and of chemical compositions given in **Table 1** was used.

2.2 Tube- End Plug Welding Procedure

Two weld joints were produced by joining the stainless steel tube to end plug autogenously using GTAW and LBW processes separately. The tube to end plug joint configuration used in the study is shown in **Fig. 1**. The welding parameters used for the GTAW weld joint are given in **Table 2**. The laser welding was carried out by using pulsed Nd:YAG laser. The parameters used for the laser joint are shown in the **Table 3**. The weld joints

were qualified using Helium leak test as per ASTM E1603M which was performed to determine the leak tightness of the welds. **Fig. 2** shows the actual tube to end plug weld joints produced using GTAW and laser processes.

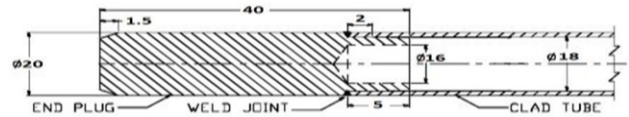


Fig. 1 : Tube to end plug configuration used in the study

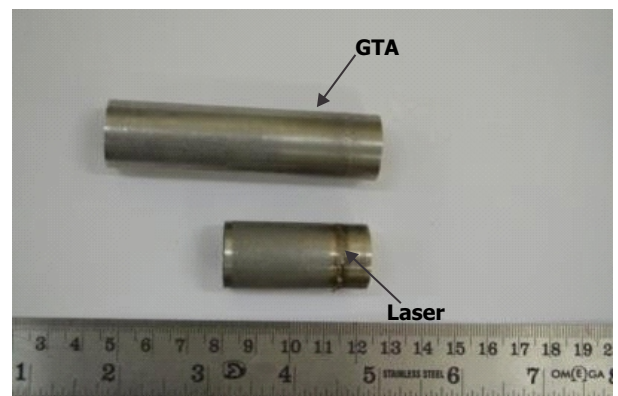


Fig. 2 : Laser and GTA welded specimens

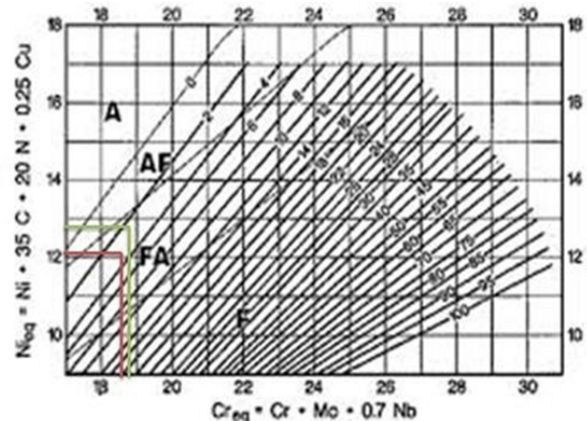


Fig. 3 : Prediction of mode of solidification for GTA weld

Table 1 : Chemical composition of the end plug and clad tube (in wt%)

Material	C	Cr	Ni	Mo	Mn	Si	P	S	Fe
End plug (SS 316L)	0.024	17.07	10.12	2.01	1.28	0.427	0.037	0.028	Balance
Tube (SS 316L)	0.015	016.41	12.59	2.26	1.75	0.52	0.033	-	Balance

Table 2 : Parameters of GTAW

Parameters	Values
Energy, J	22.05
Average Power, W	220.10
% utilization	49.6
Pulse Power, W	2500
Pulse Duration, ms	15
Frequency, Hz	10
Job rotation, rpm	1.36
Overlap	20°
Shielding gas	Argon

Table 3 : Parameters of Laser Welding

Parameters	Values
Electrode size	1.6 mm
Electrode gap	32/1000 inch
Peak Current	42 A
Start Current	30 A
Up slope	4 s
Down slope	4 s
Fixture Delay	1.6 rpm
Overlap	25%
Shielding gas	Argon

2.3 Ferrite Determination

Ferrite content of both laser and GTAW welds were determined using Magne Gage.

Predictions for Solidification Mode

Predictive constitutional diagrams like WRC 92 diagram for GTAW process and weldability diagram for laser welding was used to predict the primary mode of solidification of the welds.

2.4 Metallography

The weld joints were sectioned axially perpendicular to the weld direction and prepared for Metallography. The samples were electrolytically etched using with 10% oxalic acid solution to reveal the weld microstructure and also etched using Murakami's reagent to reveal delta ferrite exclusively. The etched samples were observed under metallurgical microscope of "Zeiss" make and scanning electron microscope (SEM). Energy Dispersive spectroscopy (EDS) analysis was performed on the welds to determine the compositions of different phases in the microstructures.

3.0 RESULTS

3.1 Delta Ferrite Content in Welds

3.1.1 GTAW Weld

Delta ferrite content and solidification mode of the weld estimated using WRC 1992 constitution diagram for the weld composition shown in **Table 1** is represented in **Fig.3**.

Chromium equivalent (Cr_{eq}) and Nickel equivalent (Ni_{eq}) were calculated using the relations given in Eq.1 and 2. The Cr_{eq} and Ni_{eq} were found to be 18.875 and 12.055 respectively. The Cr_{eq}/Ni_{eq} of the weld is 1.568. It can be observed that the predicted mode of solidification of weld is Austenite-Ferrite (AF) mode with about 2-4% ferrite content.

$$Nickel\ Equivalent\ (Ni_{eq}) = \%Ni + 35* \%C + 20* \%N + 0.25 * \%Cu \quad (1)$$

Chromium

$$Equivalent\ (Cr_{eq}) = \%Cr + \%Mo + 0.7* \%Nb \quad (2)$$

The average ferrite content in the weld was found to be 2.514. It is clear that the actual volume of delta ferrite in the GTAW weld is as predicted by the constitution diagram.

3.1.2 Laser Weld

Solidification mode of the laser weld was predicted using modified weldability diagram since cooling rate experienced by the weld is very high [6]. The chromium and nickel equivalents for laser welding have been found to be 12.2537 and 20.37 respectively using Hammer and Svensson equations (Eq. 3 and Eq. 4). The corresponding Cr_{eq}/Ni_{eq} ratio obtained is 1.66. It is found from the modified weldability diagram that Austenite-Ferrite (AF) mode of solidification is predicted for this ratio as shown in **Fig. 4** and this point lies in a region where solidification cracking is possible.

$$Nickel\ Equivalent = \%Ni + 0.31* \%Mn + 22* \%C + 14.2* \%N + \%Cu.$$

Fig. 6(b). Also, a few hot cracks were observed to be present in the weld and HAZ as shown in the **Fig. 6(c)**.

3.3 Scanning electron microscopy (SEM) and Energy Dispersive Spectroscopy (EDS)

SEM/EDS was performed on GTA and laser welds at the locations indicated in **Fig. 7** and **8**. The chemical compositions obtained from EDS are shown in **Table 4**. The same equations, Eq. (1), Eq. (2), Eq. (3) and Eq. (4) were used to calculate the Cr-Ni equivalents for GTAW and laser welds. These values were used to predict the solidification modes and cracking susceptibilities. The Cr_{eq} was calculated to be 18.92, while the Ni_{eq} was obtained as 12.9 for GTAW. It is seen to fall under AF mode of solidification with about 2-4% ferrite content according to WRC constitution diagram. In laser weld, the Cr_{eq} was found to be 16.48 while the Ni_{eq} was calculated to be 11.47 which fall in fully austenitic mode of solidification and in the cracking zone as predicted by modified weldability diagram.

4.0 DISCUSSION

4.1 Effect of Cooling Rate on Solidification Mode:

The microstructures of 316L welds made using GTAW and Laser welding processes were found to be extremely different when compared with each other. Firstly, the GTA weld consists of duplex microstructure of dendritic austenite and delta ferrite. Whereas, the laser weld consists of single phase austenite dendrites. The cooling rate of the GTA weld is of the order of 1×10^3 which was calculated using Adam's equation and

this is consistent with that reported for arc welding processes [7,8]. Whereas the cooling rate calculated for the laser weld using Adam's equations as mentioned already is 0.067×10^6 °C/s and is of the order of rapid cooling condition [8]. The difference in the microstructures of the welds made from the base materials of same composition has arisen due to a shift in the weld solidification mode to fully austenitic mode in laser weld due to rapid cooling. In GTAW weld, the duplex microstructure as shown in **Fig. 6(a)** is in agreement with that predicted using WRC -92 diagram. The retention of delta ferrite in the weld is because the solid state transformation reactions are diffusion controlled, ferrite to austenite transformation is always incomplete due to high cooling rate of the weld. Hence, the delta ferrite is retained in the weld microstructure. In laser weld, fully austenitic microstructure as shown in the **Fig. 7** is due to primary austenite mode of solidification in the weld. In austenitic stainless steel welds undergoing high rate of cooling, the solid state reactions are retarded completely giving rise to single phase microstructure [7]. The preferential solidification mode of the weld during rapid solidification such as laser welds can be explained based on the schematic of vertical section of Fe-Cr-Ni phase diagram as shown in the **Fig. 9**. The basic assumption of this theory is that the solidification is partitionless. The solidification modes for stainless steels with compositions A and B are more dependent on composition rather than cooling rate. But for stainless steel composition shown at position C close to the 316L composition, the under cooling due to rapid solidification is sufficient to bring it below both $To_{(F)}$ and $To_{(A)}$ because the difference between these lines

Table 4 : The chemical composition obtained at a point from EDS data (wt.%)

Elements	Si	P	S	Cr	Mn	Ni	Mo	Cr Eq	Ni Eq	Cr_{eq} / Ni_{eq}
Laser	0.37	0.14	0.36	15.92	1.57	10.98	-	16.475	11.46	1.4367
GTAW	0.37	0.06	-	16.90	1.79	12.20	2.02	18.92	12.9	1.466

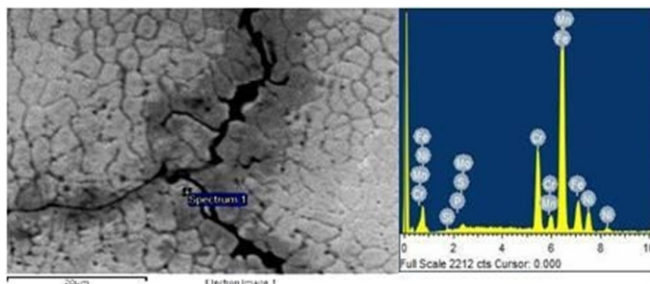


Fig.7 : EDS point scan and spectrum of laser.

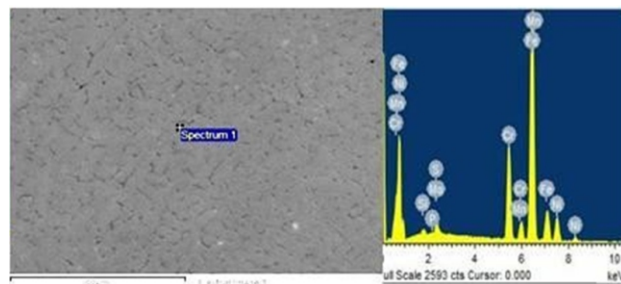


Fig. 8 : EDS point scan and spectrum of GTAW

are too low within the peritectic triangle. The solidification mode now depends on the relative kinetics of nucleation. Here the base metals in laser welds is fully austenitic. Hence, the kinetically favored solidification mode for the laser weld is primary austenite and rapid solidification suppresses the formation of delta ferrite which is in agreement with the observed microstructure. The change in the solidification mode with respect to weld cooling rate has been observed in many investigations and has been reported that the phenomenon is very sensitive for cooling rates in the order of 10^6 °C/s, comparable to that of cooling rate experienced by the laser weld experienced in the present study [8]. In our study stainless steel solidifies in austenitic mode in GTA weld also. So, cooling rate has a major effect on weld microstructure rather than solidification mode.

Suutala also concluded that cooling rate has only minor effect than the composition of the steel in determining the solidification mode [9]. But his conclusions were based on GTA welds where cooling rates were about 600°C/s which is much lower than the weld cooling rates compared in the present study. It is to be noted that the cooling rate experienced by Laser weld ($\times 10^6$) differs from GTA weld ($\times 10^3$) by order of 3.

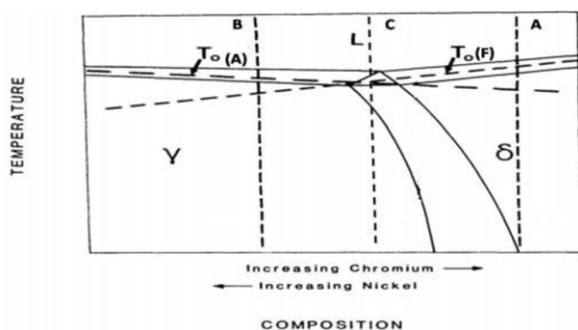


Fig. 9 : Vertical section of Fe-Cr-Ni phase diagram.

4.2 Effect of Substrate Phase on Solidification Mode

It has been found that the presence of heterogeneous nucleation sites, which are readily available in larger volume is kinetically favored phase during solidification of stainless steels with low Cr/Ni_{eq} ratio similar to that of 316L composition [8]. From the microstructures of GTA weld shown in **Fig. 5** it is quite discernable that since the base metal is predominantly austenite, the weld started solidifying epitaxially in austenitic mode and some delta ferrite is retained along the interdendritic region due to incomplete transformation. As the solidification progressed, the eutectic delta ferrite acted as precursor for the

subsequent solidification of the liquid which changed the solidification mode to primary ferrite as indicated by lacy morphology in the microstructure. It has been reported that the substrate phase from which the solidification starts acts as precursor for the solidifying phase [7]. This should be the reason for mixed mode of solidification corresponding to austenite- ferrite (AF) + ferrite-austenite (FA) in GTA weld microstructure as shown in **Fig. 5(a)**. Similarly, the laser welds also solidify from the base metal of same composition as that of GTA weld, the solidification takes place in primary austenite mode. Under rapid solidification condition, solidification is predominantly partitionless and that's the reason for only single phase austenite observed in the laser weld shown in the **Fig. 7(b)**. The observations are also in agreement with that reported by Lippold in laser welds [7].

4.3 Effect of Solidification Conditions on Solidification Mode.

Growth rate (R) can be taken as a representative factor of solidification condition which significantly changes for GTA and laser welding processes. Qualitatively, the laser weld which has higher cooling rate can be considered to have higher growth rate as compared to GTA weld. The observed solidification mode of GTA weld is austenite + ferritic (AF) whereas that of laser weld is primary austenitic which is consistent with the microstructure map constructed by Lippold summarizing the microstructures observed in stainless steels of various composition as a function of solidification rate [7]. It is clearly shown by the microstructural map that for the given steel composition, there is tendency for the weld to solidify in primary austenitic mode at higher growth rate. Therefore, the effect of solidification rate can be considered to be similar to that of the effect of cooling rate on solidification mode. In GTA weld where the growth rate varies with the same order of magnitude from the interface to the center of the weld, theoretically there should not be any variation in the solidification modes. But as observed from the microstructures it is clear that there is mixed mode of solidification (AF+FA) in the weld as discussed earlier. It can be stated that kinetics of nucleation overrides the predictions made from the constitution diagrams and maps. It can be observed from the **Fig. 5(a)** that the solidification of the GTA weld starts as coarse cellular structure and progressively changes to dendritic and then to fine dendritic. This shows that the G/R ratio is decreasing from the weld interface to the center [9]. Fluctuation of growth rate (R) in GTA weld within the same order could cause only the solidification structure and size but

not the solidification mode as the initial solidification mode is primary austenite.

4.4 Effect of Cooling Rate on Hot Cracking

It is predicted from the WRC -92 diagram and observed from weld microstructures that the weld solidification mode is primary austenite irrespective of welding process for this steel. It can be observed from the **Fig. 5(c)**, that laser weld is heavily cracked along the interdendritic regions whereas the GTA welds are free from cracks. The susceptibility to cracking for the composition of stainless steel used in this study was predicted using weldability diagram which uses Hammer and Svensson equations for GTA weld as shown in the **Fig. 10** and using modified weldability diagram for laser weld as shown in the **Fig. 4**.

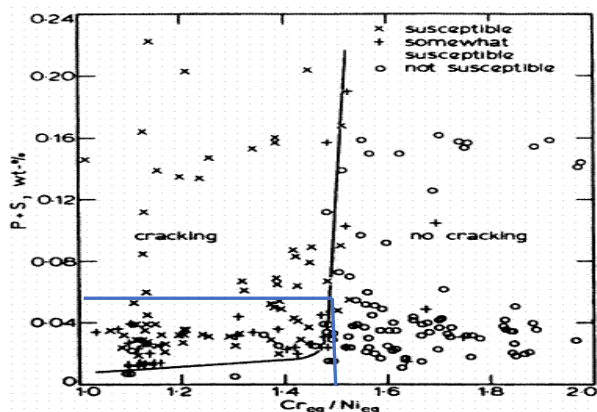


Fig 10 : Weldability diagram for cracking susceptibility of 300 series stainless steel.

The classical weldability diagram was designed for arc welding process and hence it was used to predict the susceptibility of cracking for GTA welds. It was found that the point representing the Cr_{eq}/Ni_{eq} of the stainless steel lies at the border separating cracking and no cracking region with respect to its Sulphur + Phosphorus (S+P) content. But it has been observed that the weld microstructure is devoid of any cracks. The modified weldability diagram was used for predicting the susceptibility of cracking laser welds. The diagram predicted that the primary solidification mode of the laser weld is austenite and it is highly susceptible to cracking. The prediction is in good agreement with the observed microstructure which shows several hot cracks in the weld region and HAZ. The higher cracking susceptibilities of the laser weld as compared to GTA weld can be attributed to single phase austenitic

microstructure which in turn can be attributed to rapid solidification condition. Though it is assumed that there is no segregation during rapid solidification, low melting elements such as S and P were found to be 10 times more than the nominal composition at the crack tips. Presence of high amount of impurity elements in laser welds caused hot cracking by forming low melting liquid along the interdendritic regions as shown by spot EDS analysis at the interdendritic regions in **Fig. 8**.

5.0 CONCLUSIONS

The present study was based on comparison of weld solidification structure of GTA and laser welds prepared using 316L stainless steel of same composition. The following conclusions have been drawn based on this study.

1. The solidification mode of 316L weld primarily depended on chemical composition of the stainless steel which decides the Cr/Ni_{eq} irrespective of welding process.
2. Weld cooling rate is found have profound effect on the final 316L weld microstructure. Since laser welds experience high cooling rate in the order of 10^6 °C/s, the formation of eutectic ferrite along the interdendritic regions are completely suppressed due to rapid solidification condition. This gave rise to a single phase austenitic microstructure in the laser weld. Whereas, GTA weld that experienced cooling rate in the order of 10^3 °C/s is composed of duplex microstructure of austenite and ferrite.
3. Presence of heterogeneous nucleation sites in the weld was also observed to have significant role in determining and changing the solidification mode. In laser weld, high cooling rate and epitaxial solidification of weld from austenite phase of the base metal favors austenitic mode of solidification. In GTA weld, epitaxial solidification of the weld from austenite phase of base metal favored austenite solidification mode with eutectic ferrite formed along the dendrites. Delta ferrite in the weld locally acted as preferential nucleation sites for ferritic mode of solidification which led to mixed mode of solidification in GTA weld.
4. High cooling rate, Sulphur + phosphorus impurity segregations and single phase austenitic microstructure of the laser weld led to higher cracking sensitivity than the GTA weld with duplex microstructure.

REFERENCES

1. Rafal M M, Paradowski K, Brynk T, Ciupinski L, Pakiela Z, Krzysztof J Kurzydowski (2009); Measurement of mechanical properties in a 316L stainless steel welded joint, *Int. Journal of Pressure Vessels and Piping*, (86), pp. 43-47.
2. Sarkar R, Chellapandi P, Chetal SC (2012); A design approach for establishing creep strength reduction factor for repaired welds for fast reactor fuel pin end plugs, *Nuclear Engineering and Design*, (252), pp. 192–200.
3. Petretis Br, Balciuniene M (2005); Peculiarities of laser welding of metals. *Lithuanian J Phys*, 45(1): pp. 59–69.
4. *Metals Handbook, Welding, Brazing and Soldering*, ASM, 1993. ISBN0-87170-007.
5. Kaul R, Ganesh P, Ittoop MO and Nath AK (2002); End Plug Welding of PFBR Fuel tubes with a 2.5 kW CW CO₂ Laser, *BARC Newsletter, Founder's Day Issue 2002*.
6. Lienert TJ and Lippold JC (2003); Improved weldability diagram for pulsed laser welded austenitic stainless steels, *Science and Technology of welding and joining*, pp. 1-9.
7. Lippold JC (1994); *Solidification Behavior and Cracking Susceptibility of Pulsed Laser Welds in Austenitic Stainless Steels*; *Welding Research Supplement*, pp. 129-139.
8. David SA, Vitek JM, Reed RW and Hebble TL (1987); Effect of Rapid Solidification on Stainless Steel Weld Metal Microstructures and Its Implications on Schaeffler Diagram, *Welding Research*, pp. 289-300.
9. Suutala N (1983); Effect of solidification conditions on the solidification mode in austenitic stainless steel, *Metallurgical and Materials Transactions*, pp. 191-197.

ACKNOWLEDGEMENT

The authors would like to thank members of IDEAS and MTD for their valuable contributions towards carrying out this research. The authors from SSN are thankful to IGCAR for permission to carry out the project work in IGCAR, and to SSN for their encouragement.

The present paper is a revised version of an article presented in the Young Welding Professionals International Congress (IC-2017) of the International Institute of Welding held in Chennai on December 07-09 2017 and organized by the Indian Institute of Welding.